Supporting Information

Degrees of Distortion: Synthesis, Structure and Bonding in Approximately Icosahedral $[Ru@Sn_{12}]^{4-}$ †

Sourav Mondal,[a] Ya-Shan Huang,[b‡] Zhong-Ming Sun,*[b] and John E. McGrady*[a]

S1 X-ray crystallography

Details of the crystallographic experiment are given in the main text.

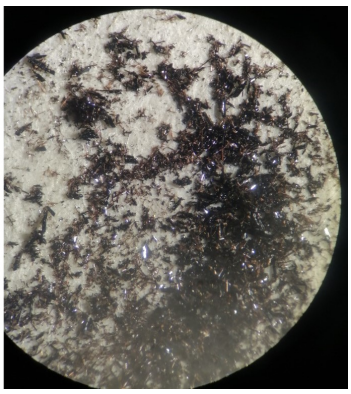

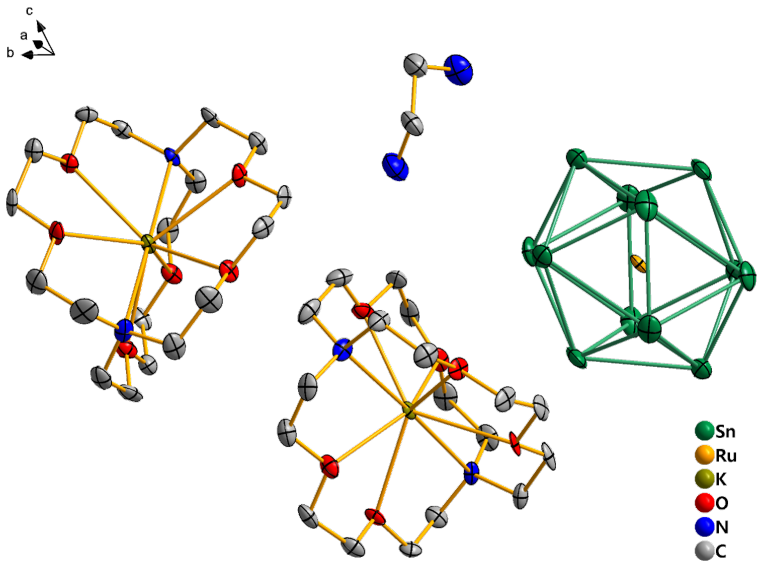

Fig. S1 Crystals of $[K(2.2.2-crypt)]_4[Ru@Sn_{12}]\cdot en$ dispersed in silicon oil and the asymmetric unit. Thermal ellipsoids are drawn at 70% probability.

S2 ESI mass spectrometry

ESI mass spectra were recorded in two solvents, acetonitrile (MeCN) and dimethylformamide (DMF). In MeCN (Figure S2), extensive fragmentation of the parent ion occurs, such that the only peaks of significant intensity correspond to $[RuSn_{10}]^-$, in isolation and as part of an ion pair with $[K(2.2.2{-}crypt)]^+$. In DMF (Figure S3), fragmentation is again observed, as is the removal of Ru from the cluster, but a peak of significant intensity corresponding to the parent ion is observed (again as an ion pair with $[K(2.2.2{-}crypt)]^+$).

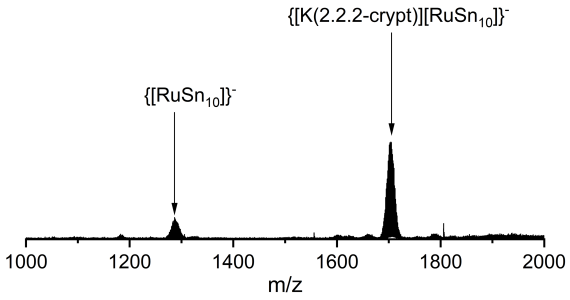

Fig. S2 ESI-MS in negative ion mode of a freshly dissolved crystalline sample of $[K(2.2.2{-}crypt)]_4[Ru@Sn_{12}]$ in acetonitrile.

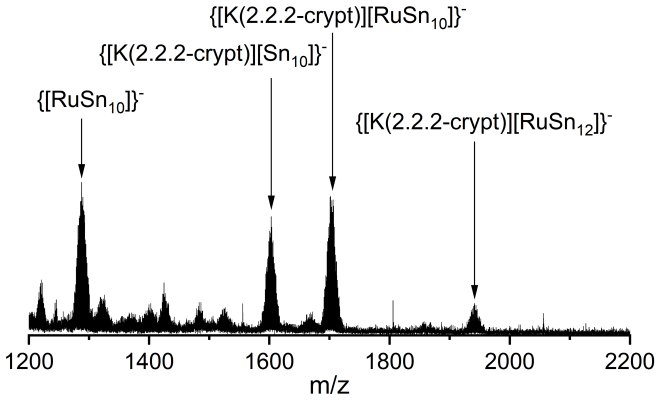

Fig. S3 ESI-MS in negative ion mode of a freshly dissolved crystalline sample of $[K(2.2.2{-}crypt)]_4[Ru@Sn_{12}]$ in dimethylformamide (DMF).

S3 Energy Dispersive X-ray (EDX) spectroscopy

The EDX spectrum in Figure S4 was measured at a single spot on the surface. The calculated elemental ratio, obtained by integration of the peaks, was 3.34:1:11.34 (K:Ru:Sn) compared to a theoretical value of 4:1:12. Deviations of this magnitude are common in Zintl clusters, where surface oxidation of the sample during measurement is difficult to avoid.

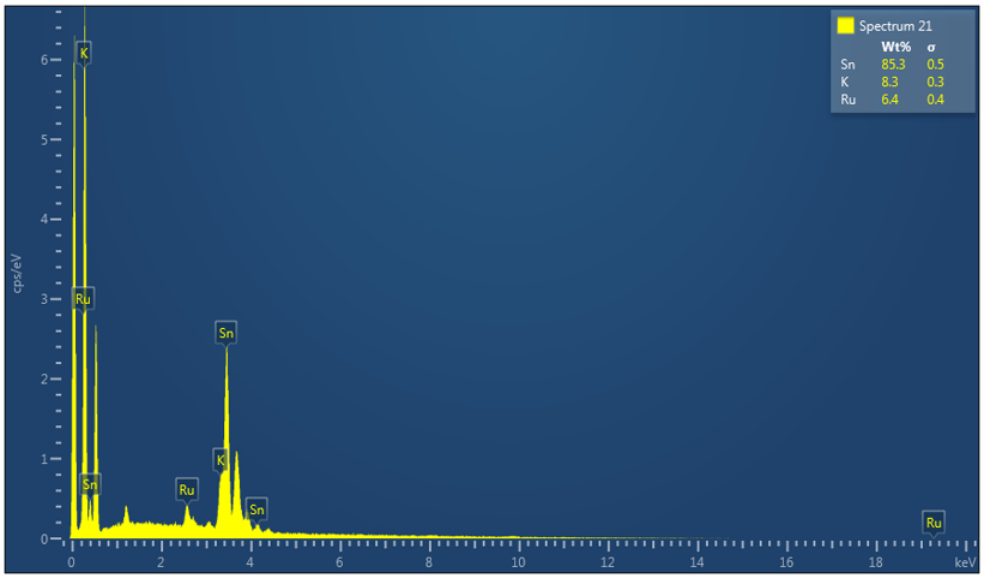

Fig. S4 EDX spectrum of $[K(2.2.2{-}crypt)]_4[Ru@Sn_{12}]$, with peaks in the ratio $K_{3.34}Ru_1Sn_{11.34}$.

S4 Computational results

Full details of the protocols used in the computational experiments are provided in the main text. For each of the clusters discussed, we have carried out a thorough analysis of the potential energy surface by initiating optimisations from a range of different, approximately icosahedral, geometries corresponding to different sub-groups of I_h. We have also considered a D_{2d}-symmetric structure, similar to that found in the crystal structure of $[Ru@Ge_{12}]^{3-}$, and also a D_{5h} bicapped pentagonal prism, similar to that reported for $[Co@Ge_{12}]^{3-}$. The results for the $[Ru@Sn_{12}]^{4-}$ cluster are shown in Table S1. Where the initial geometry corresponds to a sub-group of I_h (C_i, D_{3d}, D_{2h}, the structure relaxes back to the perfectly icosahedral one (small deviations are due to the finite convergence criterion), indicating that there is no intrinsic driving force for the experimentally observed distortion. The two geometries that are not sub-groups of I_h, D_{2d} and D_{5h}, converge on higher energy structures: D_{5h} is the more stable of the two. The energies of the different structures are plotted in Figure S5 for $[Ru@Sn_{12}]^{4-}$ as well as $[Rh@Sn_{12}]^{3-}$, $[Pd@Sn_{12}]^{2-}$, $[Tc@Sn_{12}]^{5-}$ and $[Ru@Ge_{12}]^{3-}$. In all cases, the D_{2d} isomer (red line) is taken as the energetic reference point. For $[Pd@Sn_{12}]^{2-}$, $[Rh@Sn_{12}]^{3-}$ and $[Ru@Sn_{12}]^{4-}$, the icosahedron is the most stable, and optimisations initiated from C_i, D_{2h} and D_{3d}-symmetric geometries converge back to the perfect icosahedron. However, there is a progressive destabilisation of the icosahedron relative to both D_{5h} and D_{3d} as the metal centre becomes more electron rich, to the point where the curves cross at $[Ru@Ge_{12}]^{3-}$, leaving the D_{2d}-symmetric geometry as the global minimum. The distorted variants of the icosahedron (C_i, D_{2h} and D_{3d}) are now also more stable than the most symmetric form, indicating an intrinsic instability of the I_h-symmetric form. The as-yet unknown Tc cluster $[Tc@Sn_{12}]^{5-}$ sits very close to the crossover point, and we predict that the structure of this (and also of its more synthetically tractable Re analogue) will have unusual dynamic properties as a result of the proximity of the D_{3d} and D_{2d} isomers.

Table S1 Crystallographic and DFT-optimised bond lengths, number of imaginary frequencies (N_{imag}) and relative energies (E_{rel}) of the different point groups of the $[Ru@Sn_{12}]^{4-}$ cluster.

Geometry	Ru-Sn (Å)	Sn-Sn (Å)	N_{imag}	E_{rel} (eV)
X-ray (C_i)	2.79-3.03	2.94-3.31		
		DFT-optimised		
I_h	2.96	3.11	0	0
C_i	2.95-2.96	3.11-3.12	0	0.0
D_{3d}	2.96-2.97	3.11-3.12	0	0.0
D_{2d}	3.04-3.12	2.85-2.96	0	1.07
D_{5h}	2.96-3.34	2.94-3.17	1	0.40
D_{2h}	2.96-2.96	3.11-3.12	0	0.0

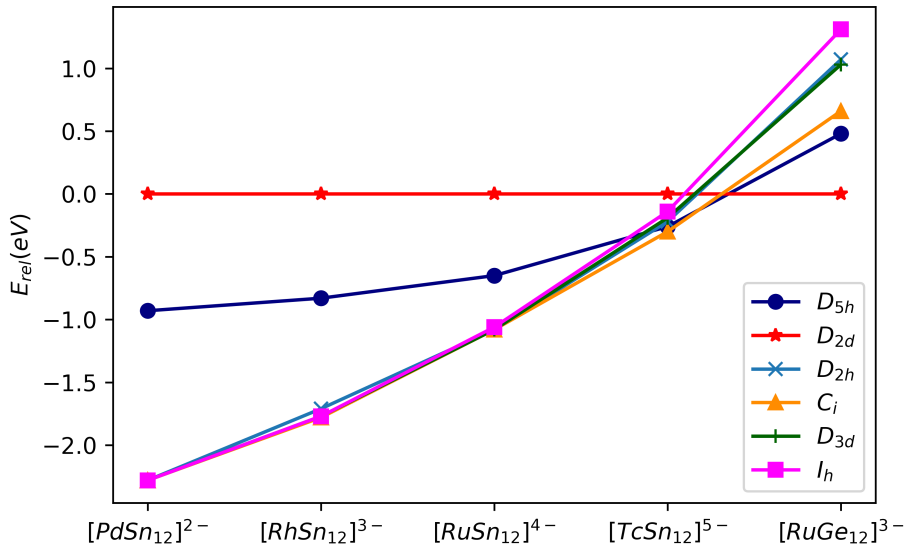

Fig. S5 Relative energy plot of different point groups of $[M@E_{12}]^{z-}$ family, w.r.t D_{2d} symmetry as a baseline. The energy differences between I_h and D_{2d} symmetric structures narrowed down along the left side of the series in the periodic table (Tc<Ru<Rh<Pd).

S4.1 Optimized Cartesian coordinates and bond energies of stationary points on the potential energy surface of the $[M@E_{12}]^{z-}$ family shown in Figure S5. All coordinates are given in Å.

Table S2 S=0 I_h-$[Ru@Sn_{12}]^{4-}$ Bond Energy: -64.280 eV

Sn	0.000000	0.000000	-2.961537
Sn	-0.000000	-0.000000	2.961537
Ru	-0.000000	0.000000	0.000000
Sn	-1.556972	2.142988	-1.324440
Sn	1.556972	-2.142988	1.324440
Sn	-2.519234	-0.818549	-1.324440
Sn	2.519234	0.818549	1.324440
Sn	2.519234	-0.818549	-1.324440
Sn	-2.519234	0.818549	1.324440
Sn	0.000000	2.648879	1.324440
Sn	-0.000000	-2.648879	-1.324440
Sn	1.556972	2.142988	-1.324440
Sn	-1.556972	-2.142988	1.324440

Table S3 S=0 D_{2d}-[Ru@Sn_{12}]$^{4-}$ Bond Energy: -63.211 eV

Ru	-0.000000	-0.000000	0.000000
Sn	-1.008956	-1.008956	2.685917
Sn	0.685818	-2.780675	1.234098
Sn	-2.780675	0.685818	1.234098
Sn	-2.780675	-0.685818	-1.234098
Sn	0.685818	2.780675	-1.234098
Sn	-1.008956	1.008956	-2.685917
Sn	2.780675	-0.685818	1.234098
Sn	-0.685818	-2.780675	-1.234098
Sn	1.008956	1.008956	2.685917
Sn	1.008956	-1.008956	-2.685917
Sn	-0.685818	2.780675	1.234098
Sn	2.780675	0.685818	-1.234098

Table S4 S=0 C_i-[Ru@Sn_{12}]$^{4-}$ Bond Energy: -64.284 eV

Sn	0.022766	-2.952047	-0.128024
Sn	-0.022766	2.952047	0.128024
Ru	0.000000	0.000000	0.000000
Sn	-1.550929	-1.232291	-2.199252
Sn	1.550929	1.232291	2.199252
Sn	-2.519268	-1.376066	0.753799
Sn	2.519268	1.376066	-0.753799
Sn	2.537923	-1.337010	0.765439
Sn	-2.537923	1.337010	-0.765439
Sn	-0.007717	1.443452	-2.585004
Sn	0.007717	-1.443452	2.585004
Sn	1.576057	-1.208492	-2.191924
Sn	-1.576057	1.208492	2.191924

Table S5 S=0 D_{3d}-[Ru@Sn_{12}]$^{4-}$ Bond Energy: -64.283 eV

Sn	1.554113	-0.897268	2.363521
Sn	-1.554113	0.897268	-2.363521
Ru	0.000000	-0.000000	0.000000
Sn	-0.000000	-2.904512	0.558118
Sn	0.000000	2.904512	-0.558118
Sn	-1.554113	-0.897268	2.363521
Sn	1.554113	0.897268	-2.363521
Sn	2.515381	1.452256	0.558118
Sn	-2.515381	-1.452256	-0.558118
Sn	-0.000000	-1.794535	-2.363521
Sn	0.000000	1.794535	2.363521
Sn	2.515381	-1.452256	-0.558118
Sn	-2.515381	1.452256	0.558118

Table S6 S=0 D_{5h}-[Ru@Sn_{12}]$^{4-}$ Bond Energy: -63.88 eV

Sn	0.000000	-0.000000	-3.339340
Sn	2.023295	-1.470010	-1.584055
Sn	2.023295	1.470010	-1.584055
Sn	-0.772830	-2.378526	-1.584055
Sn	-0.772830	2.378526	-1.584055
Sn	-2.500930	0.000000	-1.584055
Sn	0.000000	-0.000000	3.339340
Sn	2.023295	-1.470010	1.584055
Sn	2.023295	1.470010	1.584055
Sn	-0.772830	-2.378526	1.584055
Sn	-0.772830	2.378526	1.584055
Sn	-2.500930	0.000000	1.584055

Table S7 S=0 D_{3h}-[Ru@Sn_{12}]$^{4-}$ Bond Energy: -62.490 eV

Ru	0.000000	0.000000	0.000000
Sn	1.555753	-0.000000	2.520156
Sn	2.517342	1.559056	0.000000
Sn	-0.000000	2.522068	1.557341
Sn	-1.555753	0.000000	2.520156
Sn	0.000000	-2.522068	1.557341
Sn	2.517342	-1.559056	0.000000
Sn	1.555753	-0.000000	-2.520156
Sn	-0.000000	2.522068	-1.557341
Sn	-2.517342	1.559056	0.000000
Sn	-2.517342	-1.559056	0.000000
Sn	0.000000	-2.522068	-1.557341
Sn	-1.555753	0.000000	-2.520156

Table S8 S=0 I_h-[Rh@Sn_{12}]$^{4-}$ Bond Energy: -60.84 eV

Sn	-2.524070	0.820120	1.326982
Sn	-2.524070	-0.820120	-1.326982
Rh	0.000000	-0.000000	-0.000000
Sn	-1.559961	-2.147102	1.326982
Sn	1.559961	-2.147102	1.326982
Sn	-0.000000	-0.000000	2.967223
Sn	0.000000	2.653965	1.326982
Sn	2.524070	-0.820120	-1.326982
Sn	2.524070	0.820120	1.326982
Sn	1.559961	2.147102	-1.326982
Sn	-1.559961	2.147102	-1.326982
Sn	0.000000	0.000000	-2.967223
Sn	-0.000000	-2.653965	-1.326982

Table S9 S=0 D_{2d}-[Rh@Sn_{12}]$^{3-}$ Bond Energy: -59.05 eV

Rh	-0.000000	-0.000000	0.000000
Sn	-1.006508	-1.006508	2.650286
Sn	0.695579	-2.807994	1.233500
Sn	-2.807994	0.695579	1.233500
Sn	-2.807994	-0.695579	-1.233500
Sn	0.695579	2.807994	-1.233500
Sn	-1.006508	1.006508	-2.650286
Sn	2.807994	-0.695579	1.233500
Sn	-0.695579	-2.807994	-1.233500
Sn	1.006508	1.006508	2.650286
Sn	1.006508	-1.006508	-2.650286
Sn	-0.695579	2.807994	1.233500
Sn	2.807994	0.695579	-1.233500

Table S10 S=0 I_h-[Ir@Sn_{12}]$^{3-}$ Bond Energy: -62.278 eV

Sn	-2.526666	0.820964	1.328347
Sn	-2.526666	-0.820964	-1.328347
Ir	-0.000000	0.000000	0.000000
Sn	-1.561566	-2.149311	1.328347
Sn	1.561566	-2.149311	1.328347
Sn	-0.000000	-0.000000	2.970274
Sn	0.000000	2.656694	1.328347
Sn	2.526666	-0.820964	-1.328347
Sn	2.526666	0.820964	1.328347
Sn	1.561566	2.149311	-1.328347
Sn	-1.561566	2.149311	-1.328347
Sn	0.000000	0.000000	-2.970274
Sn	-0.000000	-2.656694	-1.328347

Table S11 S=0 D_{2d}-$[Ir@Sn_{12}]^{3-}$ Bond Energy: -60.67 eV

Ir	0.000000	0.000000	0.000000
Sn	-1.008869	-1.008869	2.647236
Sn	0.695977	-2.799334	1.231676
Sn	-2.799334	0.695977	1.231676
Sn	-2.799334	-0.695977	-1.231676
Sn	0.695977	2.799334	-1.231676
Sn	-1.008869	1.008869	-2.647236
Sn	2.799334	-0.695977	1.231676
Sn	-0.695977	-2.799334	-1.231676
Sn	1.008869	1.008869	2.647236
Sn	1.008869	-1.008869	-2.647236
Sn	-0.695977	2.799334	1.231676
Sn	2.799334	0.695977	-1.231676

Table S12 S=0 I_h-$[Pd@Pb_{12}]^{2-}$ Bond Energy: -51.580 eV

Pb	-2.632720	0.855423	1.384103
Pb	-2.632720	-0.855423	-1.384103
Pd	-0.000000	0.000000	0.000000
Pb	-1.627111	-2.239526	1.384103
Pb	1.627111	-2.239526	1.384103
Pb	-0.000000	-0.000000	3.094948
Pb	0.000000	2.768206	1.384103
Pb	2.632720	-0.855423	-1.384103
Pb	2.632720	0.855423	1.384103
Pb	1.627111	2.239526	-1.384103
Pb	-1.627111	2.239526	-1.384103
Pb	0.000000	0.000000	-3.09494
Pb	-0.000000	-2.768206	-1.38410

Table S13 S=0 D_{2d}-$[Pd@Pb_{12}]^{2-}$ Bond Energy: -47.87 eV

Pd	-0.000000	-0.000000	0.000000
Pb	-1.064309	-1.064309	2.731193
Pb	0.749748	-2.973557	1.284381
Pb	-2.973557	0.749748	1.284381
Pb	-2.973557	-0.749748	-1.284381
Pb	0.749748	2.973557	-1.284381
Pb	-1.064309	1.064309	-2.731193
Pb	2.973557	-0.749748	1.284381
Pb	-0.749748	-2.973557	-1.284381
Pb	1.064309	1.064309	2.731193
Pb	1.064309	-1.064309	-2.731193
Pb	-0.749748	2.973557	1.284381
Pb	2.973557	0.749748	-1.284381

Table S14 S=0 D_{2d}-$[Pd@Pb_{12}]^{2-}$ Bond Energy: -53.84 eV

Pb	1.626810	-2.239112	1.383847
Pb	2.632234	-0.855265	-1.383847
Pt	0.000000	0.000000	-0.000000
Pb	2.632234	0.855265	1.383847
Pb	0.000000	2.767694	1.383847
Pb	-0.000000	-0.000000	3.094376
Pb	-1.626810	-2.239112	1.383847
Pb	-1.626810	2.239112	-1.383847
Pb	-2.632234	0.855265	1.383847
Pb	-2.632234	-0.855265	-1.383847
Pb	-0.000000	-2.767694	-1.383847
Pb	0.000000	0.000000	-3.094376
Pb	1.626810	2.239112	-1.383847

Table S15 S=0 D_{2d}-$[Pd@Pb_{12}]^{2-}$ Bond Energy: -50.33 eV

Pt	0.000000	0.000000	0.000000
Pb	-1.062385	-1.062385	2.735219
Pb	0.741884	-2.955555	1.279614
Pb	-2.955555	0.741884	1.279614
Pb	-2.955555	-0.741884	-1.279614
Pb	0.741884	2.955555	-1.279614
Pb	-1.062385	1.062385	-2.735219
Pb	2.955555	-0.741884	1.279614
Pb	-0.741884	-2.955555	-1.279614
Pb	1.062385	1.062385	2.735219
Pb	1.062385	-1.062385	-2.735219
Pb	-0.741884	2.955555	1.279614
Pb	2.955555	0.741884	-1.279614

Table S16 S=1/2 I_h-$[Ru@Ge_{12}]^{3-}$ Bond Energy: -68.20 eV

Ru	0.000000	-0.000000	-0.000000
Ge	-2.265901	0.736236	1.191255
Ge	0.000000	2.382509	1.191255
Ge	-0.000000	-0.000000	2.663726
Ge	-1.400404	1.927490	-1.191255
Ge	-1.400404	-1.927490	1.191255
Ge	-2.265901	-0.736236	-1.191255
Ge	2.265901	-0.736236	-1.191255
Ge	-0.000000	-2.382509	-1.191255
Ge	1.400404	1.927490	-1.191255
Ge	2.265901	0.736236	1.191255
Ge	0.000000	0.000000	-2.663726
Ge	1.400404	-1.927490	1.191255

Table S17 S=1/2 D_{2d}-$[Ru@Ge_{12}]^{3-}$ Bond Energy: -69.48 eV

Ru	0.000000	0.000000	0.000000
Ge	-0.876035	-0.876035	2.491951
Ge	0.561461	-2.413503	1.114482
Ge	-2.413503	0.561461	1.114482
Ge	-2.413503	-0.561461	-1.114482
Ge	0.561461	2.413503	-1.114482
Ge	-0.876035	0.876035	-2.491951
Ge	2.413503	-0.561461	1.114482
Ge	-0.561461	-2.413503	-1.114482
Ge	0.876035	0.876035	2.491951
Ge	0.876035	-0.876035	-2.491951
Ge	-0.561461	2.413503	1.114482
Ge	2.413503	0.561461	-1.114482

Table S18 S=1 I_h-$[Mn@Pb_{12}]^{3-}$ Bond Energy: -56.74 eV

Mn	0.000000	-0.000000	0.000000
Pb	-1.625021	-2.236650	1.382326
Pb	-2.629340	0.854324	1.382326
Pb	0.000000	0.000000	3.090974
Pb	-2.629340	-0.854324	-1.382326
Pb	1.625021	-2.236650	1.382326
Pb	0.000000	-2.764651	-1.382326
Pb	1.625021	2.236650	-1.382326
Pb	2.629340	-0.854324	-1.382326
Pb	-1.625021	2.236650	-1.382326
Pb	-0.000000	2.764651	1.382326
Pb	-0.000000	-0.000000	-3.090974
Pb	2.629340	0.854324	1.382326

Table S19 S=1 D_{2h}-$[Mn@Pb_{12}]^{3-}$ Bond Energy: -57.390 eV

Mn	0.000000	0.000000	0.000000
Pb	1.572265	0.000000	2.435467
Pb	2.525207	1.853549	0.000000
Pb	-0.000000	2.917277	1.581847
Pb	-1.572265	-0.000000	2.435467
Pb	0.000000	-2.917277	1.581847
Pb	2.525207	-1.853549	0.000000
Pb	1.572265	0.000000	-2.435467
Pb	-0.000000	2.917277	-1.581847
Pb	-2.525207	1.853549	0.000000
Pb	-2.525207	-1.853549	0.000000
Pb	0.000000	-2.917277	-1.581847
Pb	-1.572265	-0.000000	-2.435467

Table S20 S=1 D_{3d}-$[Mn@Pb_{12}]^{3-}$ Bond Energy: -57.410 eV

Mn	0.000000	-0.000000	0.000000
Pb	2.479359	-1.431459	-0.682495
Pb	-0.000000	-1.822406	-2.750765
Pb	1.578250	0.911203	-2.750765
Pb	2.479359	1.431459	0.682495
Pb	1.578250	-0.911203	2.750765
Pb	0.000000	-2.862917	0.682495
Pb	-2.479359	-1.431459	-0.682495
Pb	-1.578250	0.911203	-2.750765
Pb	-0.000000	2.862917	-0.682495
Pb	0.000000	1.822406	2.750765
Pb	-1.578250	-0.911203	2.750765
Pb	-2.479359	1.431459	0.682495

Table S21 S=1; D_{2d}-$[Mn@Pb_{12}]^{3-}$ Bond Energy: -53.36 eV

Mn	-0.000000	0.000000	0.000000
Pb	-1.068436	-1.068436	3.049621
Pb	0.659375	-2.851650	1.337146
Pb	-2.851650	0.659375	1.337146
Pb	-2.851650	-0.659375	-1.337146
Pb	0.659375	2.851650	-1.337146
Pb	-1.068436	1.068436	-3.049621
Pb	2.851650	-0.659375	1.337146
Pb	-0.659375	-2.851650	-1.337146
Pb	1.068436	1.068436	3.049621
Pb	1.068436	-1.068436	-3.049621
Pb	-0.659375	2.851650	1.337146
Pb	2.851650	0.659375	-1.337146

Table S22 S=1 I_h-$[Au@Pb_{12}]^{3-}$ Bond Energy: -51.04 eV

Au	0.000000	-0.000000	-0.000000
Pb	-2.677553	-0.869990	-1.407673
Pb	2.677553	0.869990	1.407673
Pb	1.654819	2.277663	-1.407673
Pb	-1.654819	-2.277663	1.407673
Pb	-1.654819	2.277663	-1.407673
Pb	1.654819	-2.277663	1.407673
Pb	0.000000	-2.815346	-1.407673
Pb	-0.000000	2.815346	1.407673
Pb	2.677553	-0.869990	-1.407673
Pb	-2.677553	0.869990	1.407673
Pb	-0.000000	-0.000000	-3.147653
Pb	0.000000	0.000000	3.147653

Table S23 S=0 D_{3d}-$[Au@Pb_{12}]^{3-}$
; Bond Energy: -51.70 eV

Au	0.000000	0.000000	0.000000
Pb	1.801030	1.039825	2.366426
Pb	-1.801030	-1.039825	-2.366426
Pb	0.000000	2.079650	-2.366426
Pb	-0.000000	-2.079650	2.366426
Pb	2.662611	1.537259	-0.783086
Pb	-2.662611	-1.537259	0.783086
Pb	-1.801030	1.039825	2.366426
Pb	1.801030	-1.039825	-2.366426
Pb	-2.662611	1.537259	-0.783086
Pb	2.662611	-1.537259	0.783086
Pb	0.000000	3.074518	0.783086
Pb	-0.000000	-3.074518	-0.783086

Table S24 S=0 D_{5d}-$[Au@Pb_{12}]^{3-}$ Bond Energy: -51.11 eV

Au	-0.000000	-0.000000	0.000000
Pb	2.646357	0.859853	1.464235
Pb	-2.646357	-0.859853	-1.464235
Pb	-2.646357	0.859853	1.464235
Pb	2.646357	-0.859853	-1.464235
Pb	0.000000	2.782544	1.464235
Pb	-0.000000	-2.782544	-1.464235
Pb	1.635538	-2.251125	1.464235
Pb	-1.635538	2.251125	-1.464235
Pb	-1.635538	-2.251125	1.464235
Pb	1.635538	2.251125	-1.464235
Pb	-0.000000	-0.000000	3.168102
Pb	0.000000	0.000000	-3.168102

Table S25 S=0 D_{2d}-$[Au@Pb_{12}]^{3-}$ Bond Energy: -48.96 eV

Au	-0.000000	0.000000	0.000000
Pb	1.093696	1.093696	2.555229
Pb	-0.784266	3.130288	1.252527
Pb	3.130288	-0.784266	1.252527
Pb	3.130288	0.784266	-1.252527
Pb	-0.784266	-3.130288	-1.252527
Pb	1.093696	-1.093696	-2.555229
Pb	-3.130288	0.784266	1.252527
Pb	0.784266	3.130288	-1.252527
Pb	-1.093696	-1.093696	2.555229
Pb	-1.093696	1.093696	-2.555229
Pb	0.784266	-3.130288	1.252527
Pb	-3.130288	-0.784266	-1.252527

Table S26 S=0 I_h-$[Pd@Sn_{12}]^{2-}$ Bond Energy: -64.280 eV

Sn	-2.544806	0.826857	1.337883
Sn	-2.544806	-0.826857	-1.337883
Pd	0.000000	-0.000000	-0.000000
Sn	-1.572776	-2.164741	1.337883
Sn	1.572776	-2.164741	1.337883
Sn	0.000000	0.000000	2.991598
Sn	-0.000000	2.675767	1.337883
Sn	2.544806	-0.826857	-1.337883
Sn	2.544806	0.826857	1.337883
Sn	1.572776	2.164741	-1.337883
Sn	-1.572776	2.164741	-1.337883
Sn	-0.000000	-0.000000	-2.991598
Sn	0.000000	-2.675767	-1.337883

Table S27 S=0 D_{2d}-$[Pd@Sn_{12}]^{2-}$ Bond Energy: -52.33 eV

Pd	0.000000	0.000000	0.000000
Sn	-1.009938	-1.009938	2.641598
Sn	0.706718	-2.840919	1.242902
Sn	-2.840919	0.706718	1.242902
Sn	-2.840919	-0.706718	-1.242902
Sn	0.706718	2.840919	-1.242902
Sn	-1.009938	1.009938	-2.641598
Sn	2.840919	-0.706718	1.242902
Sn	-0.706718	-2.840919	-1.242902
Sn	1.009938	1.009938	2.641598
Sn	1.009938	-1.009938	-2.641598
Sn	-0.706718	2.840919	1.242902
Sn	2.840919	0.706718	-1.242902

Table S28 S=0 I_h-$[Tc@Sn_{12}]^{5-}$ Bond Energy: -67.74 eV

Sn	0.000000	0.000000	-2.968859
Sn	-0.000000	-0.000000	2.968859
Tc	-0.000000	0.000000	0.000000
Sn	-1.560821	2.148286	-1.327714
Sn	1.560821	-2.148286	1.327714
Sn	-2.525462	-0.820572	-1.327714
Sn	2.525462	0.820572	1.327714
Sn	2.525462	-0.820572	-1.327714
Sn	-2.525462	0.820572	1.327714
Sn	0.000000	2.655428	1.327714
Sn	-0.000000	-2.655428	-1.327714
Sn	1.560821	2.148286	-1.327714
Sn	-1.560821	-2.148286	1.327714

Table S29 S=0 D_{2d}-$[Tc@Sn_{12}]^{5-}$ Bond Energy: -67.59 eV

Tc	-0.000000	-0.000000	0.000000
Sn	-1.013282	-1.013282	2.750979
Sn	0.671979	-2.757701	1.241604
Sn	-2.757701	0.671979	1.241604
Sn	-2.757701	-0.671979	-1.241604
Sn	0.671979	2.757701	-1.241604
Sn	-1.013282	1.013282	-2.750979
Sn	2.757701	-0.671979	1.241604
Sn	-0.671979	-2.757701	-1.241604
Sn	1.013282	1.013282	2.750979
Sn	1.013282	-1.013282	-2.750979
Sn	-0.671979	2.757701	1.241604
Sn	2.757701	0.671979	-1.241604